Resonant transport of light from planar polymer waveguide into liquid-crystal microcavity

V. S. R. Jampani,[1] M. Humar,[1] and I. Muševič[1,2]*

[1] *J. Stefan Institute, Jamova 39, SI-1000, Ljubljana, Slovenia*
[2] *Faculty of Mathematics and Physics, University of Ljubljana, Jadranska 19, SI-1000, Ljubljana, Slovenia*

**igor.musevic@ijs.si*

http://www.softmatter.si/

Abstract: We demonstrate the resonant transfer of light from a planar waveguide to a nematic liquid-crystal microdroplet immersed in water. A wide spectrum of light from a supercontinuum laser source is coupled into a high-refractive-index polymer waveguide using a prism-film coupler. The waveguide is in contact with a water dispersion of droplets from the nematic liquid-crystal 5CB. The evanescent field of the light in the waveguide is resonantly coupled to the whispering-gallery mode resonances, sustained by $5-20\,\mu$m-sized nematic liquid-crystal droplets, which are in close proximity to the waveguide. The resonant transfer of light is tuned by the temperature-induced shifting of the WGM resonances due to the temperature dependence of the refractive index of the nematic liquid crystal. The measurements are compared to the calculations of the coupled-mode theory.

OCIS codes: (130.5460) Polymer waveguides; (140.3948) Microcavity devices; (230.3720) Liquid-crystal devices; (230.4555) Coupled resonators; (230.7400) Waveguides, slab.

References and links

1. W. Bogaerts, P. de Heyn, T. van Vaerenbergh, K. De Vos, S. K. Selvaraja, T. Claes, P. Dumon, P. Bienstman, D. van Thourhout, and R. Baets, "Silicon microring resonators," Laser Photonics Rev. **6**, 47–73 (2012).
2. D. J. W. Klunder, E. Krioukov, T. van der Veen, H. F. Bulthuis, G. Sengo, C. Otto, H. J. W. M. Hoekstra, and A. Driessen, "Vertically and laterally waveguide-coupled cylindical microresonators in Si_3N_4 on SiO_2 technology," Appl. Phys. B **73**, 603–608 (2001).
3. I. Muševič, M. Škarabot, U. Tkalec, M. Ravnik, and S. Žumer, "Two-dimensional nematic colloidal crystals self-assembled by topological defects," Science **313**, 954–958 (2006).
4. A. Nych, U. Ognysta, M. Škarabot, M. Ravnik, S. Žumer, and I. Muševič, "Assembly and control of 3D nematic dipolar colloidal crystals," Nat. Commun. **4**,1489 (2013).
5. M. Humar, M. Ravnik, S. Pajk, and I. Muševič, "Electrically tunable liquid crystal optical microresonators," Nat. Photonics **3**, 595–600 (2009).
6. M. Humar and I. Muševič, "Surfactant sensing based on whispering-gallery-mode lasing in liquid-crystal microdroplets," Opt. Express **19**, 19836–19844 (2011).
7. M. Humar and I. Muševič, "3D microlasers from self-assembled cholesteric liquid-crystal microdroplets," Optics Express **18**, 26995–27003 (2010).
8. D. J. Gardiner, S. M. Morris, P. J. W. Hands, C. Mowatt, R. Rutledge, T. D. Wilkinson, and H. J. Coles,"Paintable band-edge liquid crystal lasers," Optics Express **19**, 2432–2439 (2011).
9. G. Cipparrone, A. Mazzulla, A. Pane, R. J. Hernandez, and R. Bartolino, "Chiral self-assembled solid microspheres: A novel multifunctional microphotonic device," Adv. Mat. **23**, 5773–5778 (2011).

#191967 - $15.00 USD Received 11 Jun 2013; revised 14 Aug 2013; accepted 15 Aug 2013; published 26 Aug 2013

10. T. Araki and H. Tanaka, "Colloidal aggregation in a nematic liquid crystal: topological arrest of particles by a single-stroke disclination line," Phys. Rev. Lett. **97**, 127801–4 (2006).
11. M. Ravnik, M. Škarabot, S. Žumer, U. Tkalec, I. Poberaj, D. Babič, N. Osterman, and I. Muševič "Entangled Nematic Colloidal Dimers and Wires," Phys. Rev. Lett. **99**, 247801-4 (2007).
12. U. Tkalec, M. Ravnik, S. Čopar, S. Žumer, and I. Muševič "Reconfigurable knots and links in chiral nematic colloids," Science **333**, 62-65 (2011).
13. K. Kawano and T. Kitoh, *Introduction to Optical Waveguide Analysis* (Wiley-Interscience, 2001).
14. C. F. Bohren and D. R. Huffman, *Absorption and Scattering of Light by Small Particles* (Wiley Science, 1998).
15. H. A. Haus, W. P. Haung, S. Kawakami, and N. A. Whitaker, "Coupled mode theory of optical waveguides," J. Lightwave Technol. **5**, 16–23 (1987).
16. H. A. Haus and W. P. Haung, "Coupled-mode theory," P. IEEE **19**, 1505–1518 (1991).
17. M. J. Humphrey, E. Dale, A. T. Rosenberger, and D. K. Bandy, "Calculation of optimal fiber radius and whispering-gallery mode spectra for a fiber-coupled microsphere," Opt. Commun. **271**, 124–131 (2007).
18. S. M. Spillane, T. J. Kippenberg, O. J. Painter, and K. J. Vahala, "Ideality in a fiber-taper-coupled microresonator system for application to cavity quantum electrodynamics," Phys. Rev. Lett. **91**, 043902-1–043902-4, (2003).
19. R. Ulrich and R. Torge, "Measurement of thin film parameters with a prism coupler," Appl. Opt. **12**, 2901–2908 (1973).
20. P. K. Tien, "Light Waves in Thin Films and Integrated Optics," Appl. Opt. **10**, 2395–2413 (1971).
21. V. S. R. Jampani, M. Humar, and I. Muševič,"Resonant transfer of light from a planar waveguide into a tunable nematic liquid crystal microcavity," Proceedings of SPIE,**8642**, 86420E1-8 (2013).
22. M. Kleman and O. D. Lavrentovich, "Imperfections in focal conic domains: the role of dislocations," Phil. Mag. **86**, 4439–4458 (2006).
23. H. Stark, "Physics of colloidal dispersions in nematic liquid crystals," Phys. Rep. **351**, 387–474 (2001).
24. S.-T. Wu and K.-C. Lim, "Absorption and scattering measurements of nematic liquid crystals," Appl. Optics **26**, 1722–1727 (1987).

1. Introduction

The control of the flow of light between micro- or nano-scale objects structured on solid substrates is one of the central goals of modern photonics. Various approaches and technology platforms have been developed to achieve this aim and, among them, silicon photonics has become one of the most robust and promising platforms for future solid-state photonic circuitry [1]. To date, spatial control of the flow of light on a solid substrate is achieved either by exploiting the forbidden bands of the 2D photonic-crystalline lattice, or using total internal reflection along lithographically fabricated planar waveguides. In all cases, passive photonic waveguides have to be coupled to the active photonic micro-elements, such as optical micro-resonators, micro-lasers, modulators and detectors in a reproducible and technologically controllable way. The optical microresonators are, in most cases, realized in the form of solid-state ring resonators and the energy transfer between such an optical resonator and a planar waveguide is a generic example of the microcavity-waveguide coupling.

There are two fundamental physical requirements that have to be fulfilled simultaneously for the transfer of electromagnetic energy between a waveguide and a microcavity: (i) the EM wavefunctions in both objects must overlap spatially, (ii) the two fields must oscillate at the same frequency and they have to be phase-matched. This has serious technological implications for the gap between the two surfaces, which has to be precisely controlled to achieve an efficient energy transfer [2]. Although solid-state photonics based on precise lithography and advanced material processing and fabrication is now a superior solution on a shorter time scale, other platforms are interesting on a longer time scale because of a multitude of advantages that cannot be realized in solid-state matter, such as self-assembly, self-repair and healing. These are the advantages of soft-matter and biological systems, which are capable of self-assembly and programmable growth into fascinating photonic structures and systems, realized in living matter, for example.

It has been demonstrated in the past decade that interesting self-assembled or artificially assembled photonic structures could be realized from liquid-crystal colloids and dispersions, such as 2D [3] and 3D colloidal crystals [4], tunable micro-cavities [5], self-assembled sensors [6]

#191967 - $15.00 USD Received 11 Jun 2013; revised 14 Aug 2013; accepted 15 Aug 2013; published 26 Aug 2013

and microlasers [7–9]. It was also shown that soft matter provides complex forces of topological origin that bind micro-objects into stable super-structures [10–12]. The purpose of this work is to demonstrate the possibility of the resonant transport of light from a planar polymer waveguide into a tunable microcavity formed from a small droplet of a nematic liquid crystal. We are interested in finding the material and geometrical parameters that maximize the energy exchange of the EM waves and estimate the strength of the optical coupling of the waveguide and the microdroplet of a nematic liquid crystal (NLC).

2. Theory and Calculations

The geometry of the problem is illustrated in Fig. 1. A thin waveguide of refractive index n_s and thickness h is deposited onto a substrate of refractive index n_{sb}. A spherical micro-resonator of radius R_0 and refractive index n_c is in close vicinity to the waveguide, separated by a gap d. The waveguide and the micro-sphere are surrounded by a cladding medium of refractive index n_{cl}. The waveguide supports traveling TE and TM electromagnetic waves, which are the eigensolutions of Maxwell's equations in a planar geometry. Similarly, a spherical microresonator supports its own eigenwaves, which are corresponding solutions of Maxwell's equations in a spherical confined geometry. The confinement of electromagnetic fields is accompanied by the evanescent decay of the fields in the vicinity of the surface of the waveguide and the microresonator. When the two objects carrying their own electromagnetic fields that are eigensolutions of isolated objects start to overlap at a sufficiently small surface-to-surface separation, the eigenmodes change, because they are now the eigensolution of a coupled system of two objects. In the first-order approximation, we construct the eigensolution of the coupled system as a linear combination of the two isolated eigensolutions using a perturbative approach. This coupled-modes approach is used in many areas of physics and the corresponding mathematical formalism is well known. At the heart of the approach is the overlapping integral, which measures the extent and strength of the coupling of two isolated systems of eigensolutions.

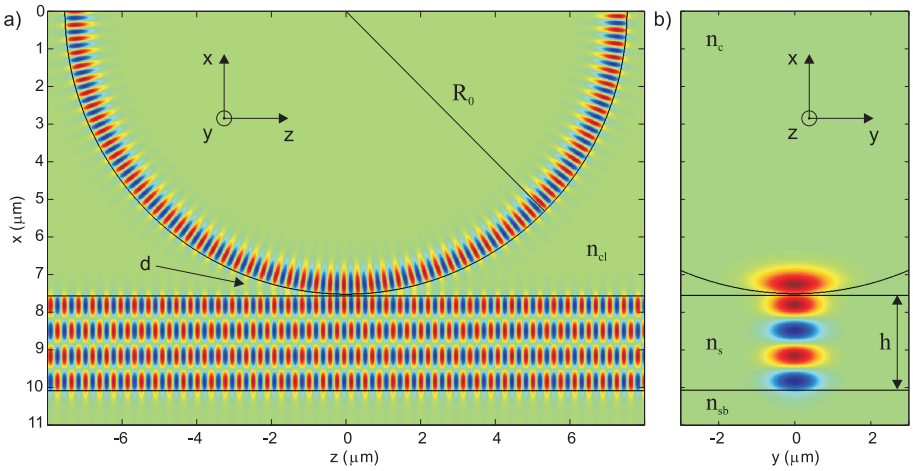

Fig. 1. Schematics of the studied system and the plot of the real part of the electric field of light in the cavity and the slab waveguide. The mode in the 15 μm-diameter cavity corresponds to the mode numbers $n = 1$ and $l = m = 125$, whereas the mode in the 2.5 μm-thick waveguide corresponds to the mode number $q = 3$. (a) Cross-section in the plane parallel to the propagation of light that goes through the point of closest separation. (b) Cross-section in the plane perpendicular to the propagation of light.

#191967 - $15.00 USD Received 11 Jun 2013; revised 14 Aug 2013; accepted 15 Aug 2013; published 26 Aug 2013

Within the coupled-modes approach one has to start with the set of eigensolutions of Maxwell's equations in a planar waveguide [13] and a spherical isotropic resonator [14], which are both well known. Without going into details, the transverse electric (TE) and transverse magnetic (TM) modes of a three-slab waveguide can be calculated by using the refractive indices of the substrate n_{sb}, a thin-film waveguide of thickness h and index n_s, surrounded by a cladding material of index n_{cl}. For a given frequency of oscillation of the EM field, there is a set of eigensolutions in the form of traveling TE or TM waves inside the thin-film waveguide that satisfy the characteristic equations. The modes are characterized by the mode number $q = \{0,1,2,..\}$; for a given set of material parameters of the waveguide, a finite number of modes with a maximum mode number q_{max} are sustained by the waveguide.

The eigenmodes of an optically isotropic microsphere are calculated by solving Maxwell's equations in spherical coordinates using the appropriate boundary conditions and are known as the whispering-gallery modes (WGMs) [14]. These modes are uniquely characterized by four mode numbers, i. e., the radial mode number n, the polar mode number l, the azimuthal mode number m and the polarization p (TE or TM). The radial mode number indicates the number of maxima in the radial intensity distribution inside the sphere; the polar mode number gives the number of wavelengths for one circulation of the light; and the azimuthal mode number indicates the inclination of the circular orbit. The radial part of the optical fields is given by the spherical Bessel function in the interior and the spherical Hankel function outside the cavity. The angular part of the eigenmodes is described by spherical harmonics. In Fig. 1 we represent the real part of the electric field distribution for the first radial WGM with $l = m$. The theory of WGMs can also be applied to the birefringent optical microcavities, such as a nematic liquid-crystal droplet with a radial internal structure [5]. In this geometry, the TE and TM WGMs of the birefringent cavity are completely decoupled; the TE mode senses the ordinary index of refraction, whereas the TM mode senses the extraordinary index.

The electromagnetic fields emanate from the surfaces of the waveguide and the microsphere and decay exponentially into the surrounding medium. The penetration lengths depend on the material parameters and are typically in the range of 100 nm. These evanescent fields are the only source of the coupling between the light fields in the waveguide and in the microcavity. Their spatial and temporal overlapping determine the degree of coupling and, therefore, also the amount of energy that can be transferred between the waveguide and the microresonator.

We are interested in elucidating the influence of the material and geometrical parameters on the energy exchange of the EM waves between a planar polymer waveguide and a small NLC droplet floating in water that is in close vicinity to the surface of the waveguide. Such an analysis is important for the future development of liquid-crystal and polymer waveguide materials, as well as technical solutions that would stabilize the gap between the waveguide and the NLC droplet to an optimum value. The degree of coupling and the efficiency of the energy transport between the waveguide and the LC droplet in the close vicinity of their surfaces was calculated approximately using the coupled-mode theory [15, 16]. Two of the most important factors to achieve an efficient coupling are the spatial overlap of the two light fields and their phase matching. The overlap of the two electric fields is characterized by calculating the integral in the (x,y) plane, which is perpendicular to the direction of propagation, z:

$$\eta_{sc(cs)}(z) = \frac{\omega\varepsilon_0}{4} N_s N_c \iint_{\text{cavity(slab)}} \left(n^2_{c(s)} - n^2_{cl}\right) \vec{E}_c \cdot \vec{E}_s \, dx \, dy. \tag{1}$$

Here, the subscripts s and c denote the slab and the cavity, respectively; N_c and N_s are normalization constants, $\vec{E}_c$ and $\vec{E}_s$ are the electric fields of the eigenmode(s) in the waveguide and microsphere. The degree of coupling is determined by the coupling coefficient κ, which is calculated by integrating $\eta_{sc(cs)}(z)$ along the propagation of light taking into account the phase

#191967 - $15.00 USD Received 11 Jun 2013; revised 14 Aug 2013; accepted 15 Aug 2013; published 26 Aug 2013

mismatch [17]

$$\kappa = \int_{-\infty}^{\infty} \sqrt{\eta_{sc}(z)\eta_{cs}(z)} \exp\left[i\big(\beta_s - \beta_{c,\mathrm{eff}}(z)\big)z\right] dz. \tag{2}$$

The overlap integral $\eta_{sc(cs)}(z)$ decreases rapidly while moving from the point of closest separation, because of the exponential decay of the fields away from the surface. At the same time, when moving from this point, the mismatch of the phases of the two light fields results in rapid spatial oscillations, which reduce the coupling efficiency. It is clear that the two propagation constants β_s and $\beta_{c,\mathrm{eff}}$ should be as close as possible to minimize the phase mismatch of the two light fields and to maximize the coupling. This is normally achieved by using an appropriate refractive index and thickness of the waveguide. More precisely, the propagation constant of the cavity $\beta_{c,\mathrm{eff}}(z)$ as seen by the slab changes while moving in the z-direction away from the point of smallest separation because of the curvature. However, this correction is small and does not change the coupling significantly. Finally, from the coupling coefficients κ_i that describe the coupling into individual waveguide modes, the total coupling can be calculated in the steady state by taking into account the buildup of light in the cavity, which interferes with the light in the waveguide. It should also be considered that the light is coupled into the cavity through a single waveguide mode, but is coupled back from the cavity to all the waveguide modes [18].

The calculations were carried out at a vacuum wavelength $\lambda_\circ \sim 600\,\mathrm{nm}$ and the TM polarization. The light was propagating in a 2.5 μm-thick polymer film of refractive index $n_s = 1.675$ in a TM mode with the mode number $q = 3$. The index of the glass substrate was $n_{sb} = 1.50$ and the index of the cladding (in this case water) was $n_{cl} = 1.33$. In the calculations, the light was tightly focused just underneath the NLC droplet. The diameter of the NLC droplet was 15 μm, the refractive indices were $n_o = 1.54$ and $n_e = 1.71$, and the Q-factor was $2.5 \cdot 10^4$. The two integrals (1) and (2) were calculated numerically.

One of the crucial parameters in the coupling experiments is the surface-to-surface separation of the waveguide and the cavity. For a given set of material and geometrical parameters, there is an optimum separation, where the coupling is a maximum. However, in our case the coupling is always relatively weak because of the thick multimode waveguide, and the experiment is expected to be in the undercoupled regime. In this regime the coupling efficiency is always increasing with an increasing coupling coefficient and therefore decreasing separation. Figure 2 shows the calculated coupling efficiency as a function of the surface-to-surface separation between the NLC microdroplet and the polymer waveguide. The coupling decreases approximately exponentially with increasing separation. This is expected, since the evanescent fields of both the cavity and the waveguide are decreasing exponentially. At zero separation we obtain 35% coupling into a single cavity mode, which is very efficient. The coupling is still substantial up to a surface separation of 200 nm, but falls essentially to zero for a separation larger than 400 nm. Because of the weak coupling coefficients the coupling to the waveguide does not have a strong effect on the cavity Q-factor. At zero separation the Q-factor is only decreased by 12%.

To find the optimum parameters for the resonant light transfer, the coupling was also calculated for different refractive indices of the waveguide and the cavity, and is shown in Fig. 3. Such an analysis is the first necessary step in the design and selection of materials to assemble photonic circuits based on soft matter. In these calculations the surface-to-surface separation was 50 nm. When the refractive index of the waveguide is small, there is just one mode in the waveguide, making it a single mode. Under this condition the coupling is a maximum, because the mode extends out of the waveguide considerably. At even smaller refractive indices, the coupling efficiency drops rapidly to zero, since the TM modes are no longer guided by the waveguide. When the index of the waveguide n_s is increased, the coupling decreases, because

#191967 - $15.00 USD Received 11 Jun 2013; revised 14 Aug 2013; accepted 15 Aug 2013; published 26 Aug 2013

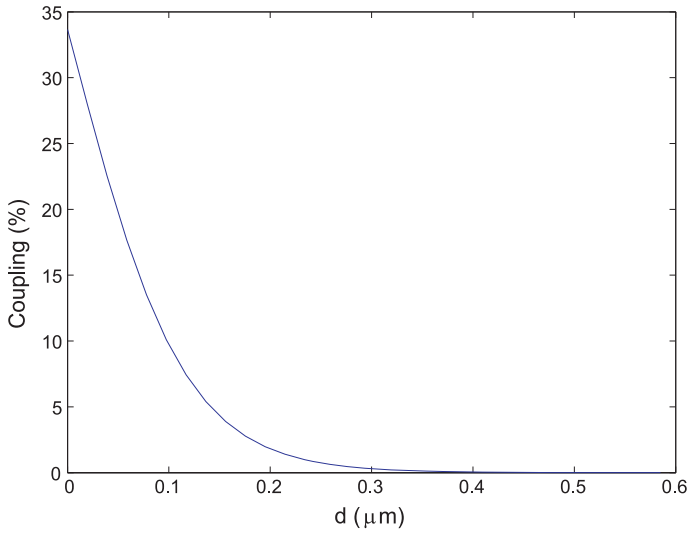

Fig. 2. Calculated coupling efficiency for NLC droplets similar to those used in the experiments, as a function of surface-to-surface separation. The coupling decreases approximately exponentially with increasing separation.

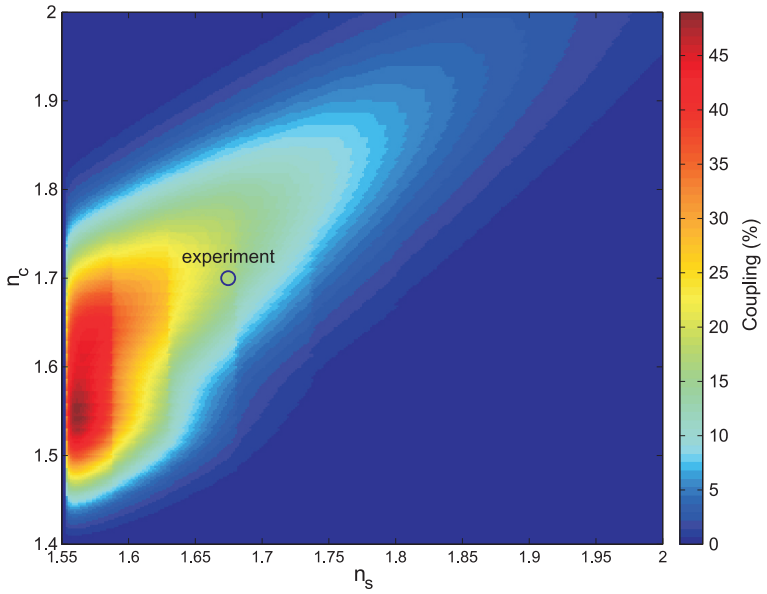

Fig. 3. Calculated coupling efficiency when changing the refractive indices of both the slab waveguide n_s and of the cavity n_c, at a surface-to-surface separation of 50 nm. The highest coupling of nearly 50% is achieved at small refractive indices of the slab, where a single-mode propagation is achieved. The refractive index of the cavity is optimum when the spatial phase matching of both light fields is a maximum. For higher indices a maximum coupling is achieved along the diagonal corresponding to the best possible phase matching. The circle shows the values of the indices of both materials (the polymer and the NLC), used in the experiment. At this point the expected coupling efficiency is $\sim$ 20%.

#191967 - $15.00 USD Received 11 Jun 2013; revised 14 Aug 2013; accepted 15 Aug 2013; published 26 Aug 2013

the mode is more confined to the waveguide and the evanescent tail is short. At even higher refractive indices more modes are guided by the waveguide. Since the light is also leaking from the cavity into these modes, the coupling is getting smaller for each new mode that appears. The effect is clearly visible in Fig. 3 as steps in the direction of increasing n_s. Increasing the waveguide index is effectively very similar to increasing its thickness and the results in both cases are very similar. The refractive index of the cavity n_c was also varied to obtain the optimal value. Maximum coupling is achieved for phase matching when the two propagation constants are equal. When the waveguide's refractive index is increased, the cavity's refractive index should also be increased to achieve good phase matching. Therefore, the maximum coupling is positioned approximately along a diagonal of the (n_s, n_c) diagram. The calculations were performed at a wavelength close to 600 nm, changing the polar mode number l of the cavity. Because the polar mode number is an integer, it can only be changed in discrete steps of 1. Therefore, there are also small steps in the direction of increasing n_c .

3. Experiments

The experiments were performed on an inverted microscope (Nikon Eclipse, TE2000-U), using the set-up shown in Fig. 4. The resonant transfer of light from a planar waveguide into a NLC microcavity was achieved using a thin polymer film as a light waveguide. A hybrid polymer (optiNDEX D1-20, Brewer sci., USA) with a high refractive index $n_s = 1.675$ was spin coated on a microscope glass slide. The thickness of the spin-coated thin film was 2.5 μm, measured using an interference method. The uniformity of the thickness of the film was better than 100 nm over the length of 70 mm. The roughness of the film was measured using a contact atomic force microscope and we found that the waveguide films are very smooth, with an RMS of just 0.2 nm. A supercontinuum laser (Fianium SC-450) was used to generate a broad spectrum of light from 450 nm to 2000 nm.

A spectral band of ~ 60 nm width could be coupled into the waveguide by using a prism-film coupler [19,20]. The transfer of light from the high-refractive-index prism into the thin polymer film can only be obtained when the propagation constant of the prism matches with one of the modes available in the thin-film waveguide [19]. The number of guided modes in the polymer film can be varied with the thickness and the refractive index of the thin film. For the vacuum

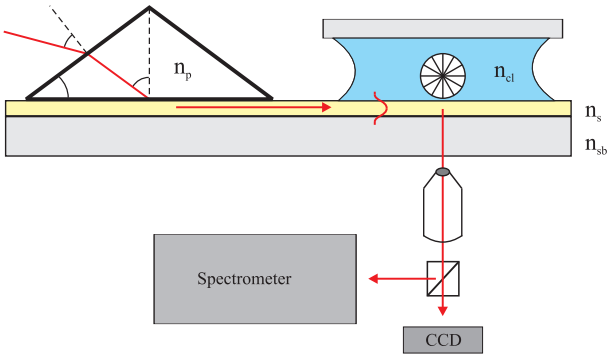

Fig. 4. Schematic diagram of the experimental set-up. The beam from the supecontimuum laser is coupled into the slab waveguide using a high-index prism coupler. The light is propagating along the polymer film into a cell containing a water dispersion of liquid-crystal droplets. Part of the light is resonantly coupled from the waveguide into the WGMs in the NLC droplets. The light emitted from the droplets is captured by a microscope objective and sent to the camera or spectrometer.

#191967 - $15.00 USD Received 11 Jun 2013; revised 14 Aug 2013; accepted 15 Aug 2013; published 26 Aug 2013

wavelength around $\lambda \sim 600\,\text{nm}$, we estimate that six modes could be guided by the polymer films, and in the experiments modes with mode numbers $q = 2...4$ were excited. On top of the waveguide the measuring cell was assembled using Mylar spacers and a microscope slide, as shown in Fig. 4.

The nematic liquid-crystal (NLC) 4-cyano-4'-pentylbiphenyl (5CB, Nematel) was mixed into a 10 mM aqueous solution of surfactant sodium dodecyl sulphate (SDS, Sigma-Aldrich). Because the NLC is immiscible with water, NLC microdroplets of various sizes are formed during mechanical stirring. These LC droplets work as tunable WGM microcavities [5], sensors [6] and in some special cases as 3D lasers [7–9], as discussed earlier. Individual NLC microdroplets were selected and observed using a $60\times$ microscope objective. We used an imaging spectophotometer with a 0.5 nm spectral resolution (Andor, Shamrock SR-500i) and an attached cooled EMCCD camera (Andor, Newton DU970N) to analyze the spectrum of light that was eventually emitted from the microdroplets [21] .

4. Results and discussion

Figures 5(a) and 5(b) show a selected 5CB microdroplet, as observed in the SDS solution using non-polarized light [Fig. 5(a)] and between crossed polarizers [Fig. 5(b)]. The interior of the droplets is free of structural defects, except for the $+1$ radial hedgehog defect in the droplet's center [22, 23]. The polarized image [Fig. 5(b)] indicates a good radial distribution of the NLC with the director field pointing perpendicularly from the surface into the center of the droplet. When the droplets are freely floating in the SDS water solution, there is no observable light emitted from them. However, because of gravity, the droplets gradually precipitate at the bottom of the measuring cell, i.e., on the surface of the polymer waveguide. In this position, the surface-separation of the NLC droplets from the waveguide was not well defined because there was still some Brownian motion of the droplets. However, we have clearly seen that the droplets did not stick onto the polymer waveguide, and this is probably due to electrostatic repulsion by

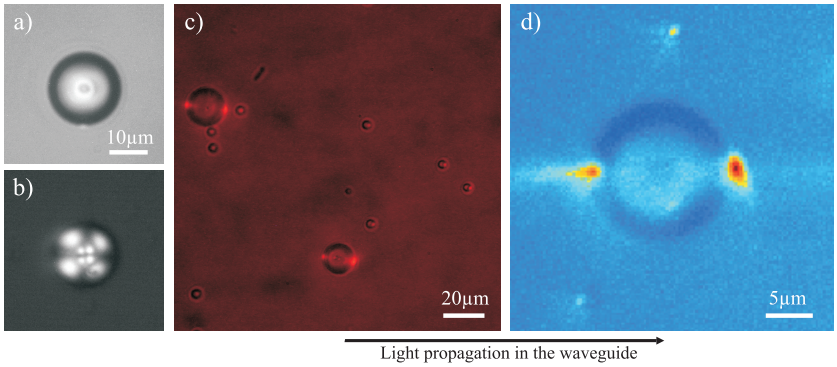

Fig. 5. Droplets of 5CB liquid-crystal in the SDS solution after they settled at the bottom of the cell, i.e., onto the polymer waveguide surface. (a) A micrograph of a single droplet with a clearly visible radial hedgehog point defect in the center. (b) The same droplet under crossed polarizers. The black cross reveals the radial configuration of the director in the droplet. (c) When light is sent through the polymer waveguide, two bright spots can be observed on each droplet. They are due to the leaking of light that is resonantly circulating inside the NLC droplet. This leakage is manifested in the two bright spots at the circumference of the droplet, aligned along the direction of propagation of light in the waveguide. Weak background light is used to see the droplets. (d) False color representation of the light intensity emitted from an individual droplet, optically coupled to the waveguide.

#191967 - $15.00 USD Received 11 Jun 2013; revised 14 Aug 2013; accepted 15 Aug 2013; published 26 Aug 2013

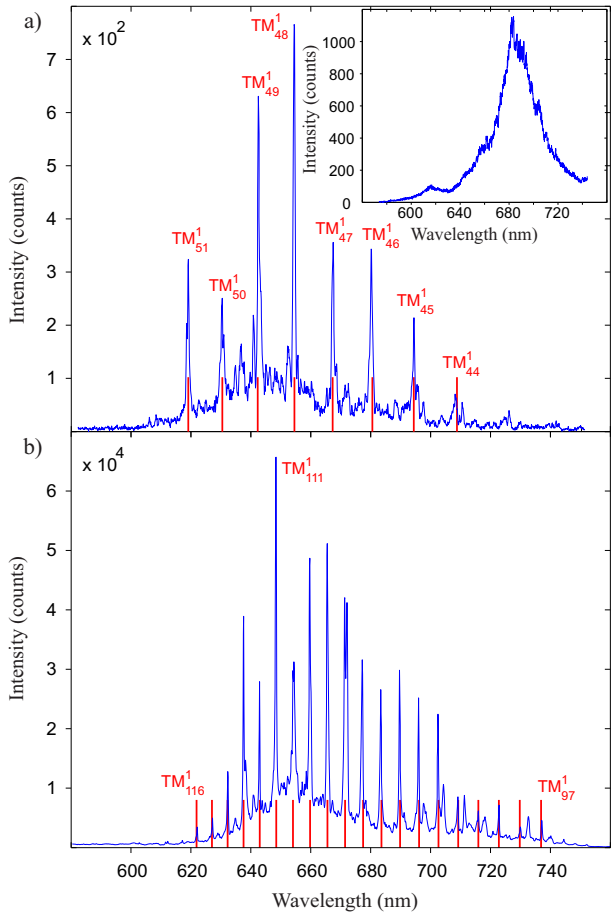

Fig. 6. (a) Spectrum of light from a 6 μm diameter NLC droplet reveals distinct equally separated peaks corresponding to WGMs in the droplet. The mode numbers and positions of the calculated modes are shown in red. The inset shows that the spectrum of light transmitted through the waveguide and measured at the end of the waveguide does not contain any sharp spectral lines. (b) Spectral lines corresponding to WGMs in a larger droplet with a diameter of 14.6 μm are more densely distributed.

surface charges, resulting from the added SDS surfactant. Although the surface separation is not known, we think that it is not larger than 100 nm, because we can clearly observe the two bright spots on the droplets, as presented in Figs. 5(c) and 5(d). These two bright spots clearly indicate that the light was transferred from the polymer waveguide into the WGM modes of the NLC microcavity. This transferred light is circulating inside the NLC droplet and because the WGMs are leaky modes, some of the light is emitted from the NLC droplet. To the observer, this leakage is manifested as two bright spots at the circumference of the droplet, clearly seen in Fig. 5(d). Note that the smaller droplets in Fig. 5(c) have only one bright spot, indicating that the light leaks out of the droplet immediately.

The spectrum of light leaking out of the NCL cavity is presented in Fig. 6 for two different diameters of the droplets. WGM resonances are clearly revealed in both cases, indicating the resonant transfer of light between the waveguide and cavity modes. All of the modes are TM polarized, because the TM polarized light is launched into the waveguide. The peaks were

#191967 - $15.00 USD Received 11 Jun 2013; revised 14 Aug 2013; accepted 15 Aug 2013; published 26 Aug 2013

fitted to the WGM solutions of an optically isotropic cavity by changing only the diameter of the droplet. The best-fitted WGM peaks are shown with vertical lines in both panels of Fig. 6. This gives us the fitted diameters of 6.51 μm and 14.19 μm. These fitted diameters match closely with the measured ones and the wavelengths of the calculated modes match perfectly with the experimental peaks. The width of the WGM resonant lines is typically 0.6 nm, which is limited by the spectrometer's resolution and sensitivity, indicating that the lower limit for the quality factor of the NLC cavity is around $Q = 1000$. The baseline of the WGM spectra is of the order of 20% of the maximum peak height, which indicates the amount of non-resonantly transferred light from the ~ 60 nm broad band of light, injected from the supercontinuum laser into the polymer waveguide. The band of light transmitted through the waveguide is shown in the inset to Fig. 6(a). The position of the coupled band is controlled by the angle of incidence onto the prism. The spectrum of the transmitted light is relatively smooth, with no sharp spectral peaks.

The tunability of the resonant light transfer between the NLC cavity and the waveguide was demonstrated by changing the temperature, as shown in Fig. 7. It clearly shows two distinct sets of WGM resonances that have the opposite temperature dependencies. The wavelengths of the first set of WGM resonances increase with increasing temperature, whereas the second set shows decreasing resonant wavelengths. The reason for this is the temperature dependence of the order parameter of the NLC and the consequent temperature dependence of both refractive indices: in the NLC the ordinary refractive index increases with increasing temperature, whereas the extraordinary index decreases with increasing temperature. This clearly indicates that the two sets of WGM resonances correspond to the TE and TM polarized WGMs. The electric field of light is in the radial direction for TM modes and senses the extraordinary index of refraction. Because this index decreases with increasing temperature, the corresponding wavelength also decreases to preserve the condition for the resonances. On the other hand, the resonant wavelengths of the TE polarized WGMs in the NLC radial microcavity increase with increasing temperature. At the temperature of the nematic-isotropic phase transition (311 K) both sets of WGMs show a discontinuity because of the first-order nature of this transition.

The total amount of light that was coupled to the NLC droplet was also measured and compared to the calculations. Only the light with a frequency and bandwidth matching a single WGM can be coupled to the cavity. The power of the light propagating in a 300 μm-wide strip in the waveguide matching this bandwidth was measured at the end of the waveguide, yielding $4 \cdot 10^{-9}$ W. The light that is resonantly coupled into the droplet is lost through different mechanisms, such as material absorbtion, bulk and surface scattering and radiative loss due to the curvature. In the NLC droplets the dominant power-loss mechanism is the scattering of light on thermally excited fluctuations of the director field. The absorbtion is much smaller compared to the scattering [24]; therefore, most of the light coupled into the droplet is also emitted by the droplet. This means that by measuring the emitted power, the coupling efficiency can be calculated. The emitted light intensity was measured by using a microscope objective and sending the captured light to the spectrometer. The amount of light emitted by the droplet through a single WGM was estimated to be $2 \cdot 10^{-12}$ W. By dividing the power emitted from the droplet by the power available in the waveguide for coupling, the coupling efficiency could be estimated to be approximately 0.05%. Such a small coupling efficiency is mainly due to the rather wide beam of light that is propagating in the waveguide, which means that most of the light is just passing by the contact area between the droplet and the waveguide, where the resonant transport is taking place. If the light would be sharply focused underneath the droplet in the same way as in the calculations, the effective coupling efficiency would increase to $\sim 10\%$. We have to emphasize that because of many assumptions made in the calculations and measurement errors, this result is only accurate to within an order of magnitude.

#191967 - $15.00 USD Received 11 Jun 2013; revised 14 Aug 2013; accepted 15 Aug 2013; published 26 Aug 2013

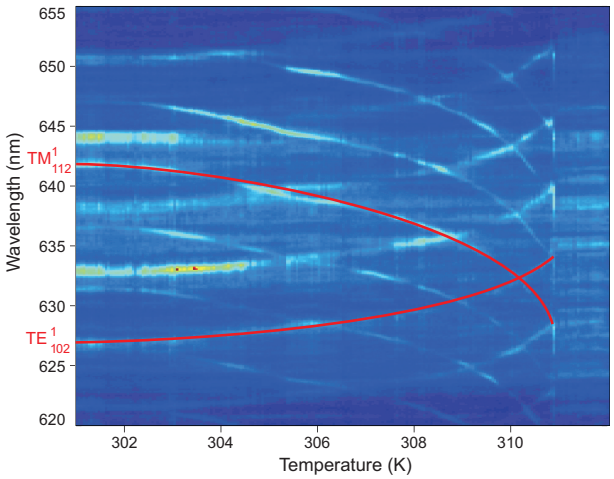

Fig. 7. Spectrum of light emitted from the same droplet as in Figure 6b as a function of temperature. Two sets of modes correspond to the TM (decreasing resonant wavelengths with increasing temperature) and TE polarizations (increasing resonant wavelengths) of the WGMs in the birefringent NLC microcavity. At 311 K the birefringent nematic phase melts into the isotropic liquid phase. The two solid lines represent the modes TM^1_{112} and TE^1_{102}, and are just guides to the eye.

The comparison of this estimated experimental value and the theory is represented by a circle in Fig. 3 and corresponds to a coupling efficiency of $\sim 20\%$. Taking into account the experimental errors, the measured coupling efficiency matches quite well with the calculated result. At a fixed refractive index n_s of the polymer waveguide, the experiment is not far from the optimal coupling regime. However, it is clear from Fig. 3 that much better light transfer could be obtained by decreasing both refractive indices: the refractive index of the cavity (n_c) should be decreased to 1.55 and the refractive index of the waveguide should also be around 1.55 to make the waveguide single-mode. Finally, to increase the level of light that is resonantly transferred into the NLC cavity, the light in the waveguide should be much tightly focused at the contact area. This could be achieved either by external focusing of light or by using structured and tapered planar waveguides.

5. Conclusions

We have demonstrated the resonant transfer of light from a planar polymer waveguide into a liquid-crystal microdroplet, acting as a birefringent WGM cavity. The demonstration is compared to the calculations of light transfer within coupled-mode theory. It shows that material optimization, such as tuning the refractive indices of the waveguide and the cavity, could substantially improve the performance of the device. Our results confirm the proof-of-principle that soft matter photonic microelements, such as self-assembled microcavities and lasers based on liquid crystals, could be used for advanced photonic applications such as frequency filtering, optical switching and sensors.

Acknowledgements
This work was supported by the European Commission Marie Curie project HIERARCHY grant PITN-GA-2008-215851 (V.S.R.J.), the Slovenian Research Agency (ARRS) contracts P1-0099 and J1-3612 (M.H., I.M.), and in part by the Center of excellence NAMASTE (I.M.).

#191967 - $15.00 USD Received 11 Jun 2013; revised 14 Aug 2013; accepted 15 Aug 2013; published 26 Aug 2013